



Contents lists available at ScienceDirect

## Arabian Journal of Chemistry

journal homepage: [www.ksu.edu.sa](http://www.ksu.edu.sa)

# Anti-TMV activity of flavonol derivatives containing piperidine sulfonamide: Design, synthesis, mechanism study

Zhiling Sun, Wei Zeng, Qing Zhou, Yujiao Qiu, Yuzhi Hu, Jieyu Li, Hong Fu, Hongqian Zou, Wei Xue\*

State Key Laboratory of Green Pesticide, Key Laboratory of Green Pesticide and Agricultural Bioengineering, Ministry of Education, Center for R&D of Fine Chemicals of Guizhou University, Guiyang, 550025, China

## ARTICLE INFO

## Keywords:

Flavonol  
Piperidine sulfonamide  
Antiviral activity  
Molecular docking  
Biosecurity

## ABSTRACT

A series of flavonol derivatives containing piperidine sulfonamide were designed and synthesized. The EC<sub>50</sub> values for the curative of tobacco mosaic virus (TMV) by **Z6** and **Z22** were 108.2 and 102.7 μg/mL, respectively, outperforming the control agent ningenmycin (NNM) with an EC<sub>50</sub> value of 253.8 μg/mL. Additionally, the EC<sub>50</sub> values for the protective activity of **Z6** and **Z21** were 100.9 and 123.2 μg/mL, respectively, also surpassing the control agent NNM with an EC<sub>50</sub> value of 203.7 μg/mL. Microscale thermophoresis (MST) and molecular docking test showed that **Z6** bound well with tobacco mosaic virus coat protein (TMV-CP). The biological safety test showed that **Z6** had almost no effect on seed germination and seedling growth. After treatment with **Z6**, the chlorophyll content and superoxide dismutase (SOD) activity in tobacco leaves increased, while the malondialdehyde (MDA) content decreased. Therefore, **Z6** has a high probability as a potential antiviral agent.

## 1. Introduction

Plants contribute to over 80 % of the Earth's biomass, thus playing a crucial role in the functioning and stability of ecosystems. However, plant viruses significantly diminish the yield and quality of important agricultural crops, leading to substantial damage to key cash crops (Keim and Alavanja, 2001; Zhang et al., 2024). As the earliest discovered non-cellular infectious agent, TMV has paved the way for human to study the field of plant virology (Jones, 2021; Kosamu et al., 2020; Li et al., 2022). But TMV is a single-stranded RNA virus with a unique one-dimensional structure and nanoscale monodispersity, which can infect 9 plant families and hundreds of plant species, including tobacco, orchids and tomatoes. Especially for important sources of cash crops and the provinces of tobacco production, TMV has a huge impact (Ilyas et al., 2022; Liu et al., 2015; Pan et al., 2023). Upon infection, a plant must not rely solely on its endogenous immune system for defense. At present, chemical pesticide preparations are used as the main means to control plant viruses. The common anti-plant virus control agents mainly include NNM and ribavirin, but their long-term excessive use will also

cause resistance to plant viruses (Zhou et al., 2024; Cao et al., 2023a; Wang et al., 2024). Therefore, it is very important to develop a green and efficient compound for the prevention and cure of TMV.

Flavonols, widely distributed in nature, they are a class of plant secondary metabolites, that exist in red wine, coffee, tea, raspberry, ginkgo biloba and different medicinal materials (Aherne and O'Brien, 2002; Nimptsch et al., 2016; Kakigi et al., 2012), and play an important ecological role. Existing studies have shown that flavonols have a wide range of biological activities such as antibacterial (Meng et al., 2023; Gong et al., 2024a), insecticidal (Borsari et al., 2016; Shamshad et al., 2020; Landi et al., 2020), antiviral (Chen et al., 2021) and anti-tumor (Shi et al., 2014; Li et al., 2016; Du et al., 2016) effects, which have paved a new bridge for the development of green pesticides and the combination of natural products. In addition, piperidine ring fragments also have good physiological and pharmacological activities (Ding et al., 2020; Wang et al., 2023a; Zhang et al., 2019), so they play an important role in the process of creating medicine and pesticides. Sulfonamide compounds, when used as intermediates, have antibacterial (Chen et al., 2023; Meseli et al., 2021; Wu et al., 2022; Mao et al., 2024), antiviral

**Abbreviations:** <sup>1</sup>H NMR, <sup>1</sup>H nuclear magnetic resonance; <sup>13</sup>C NMR, <sup>13</sup>C nuclear magnetic resonance; <sup>19</sup>F NMR <sup>19</sup>F, nuclear magnetic resonance; HRMS, High-resolution mass spectrometry; TMV, Tobacco mosaic virus; EC<sub>50</sub>, Median effective concentration; DMSO, Dimethylsulfoxide; NNM, Ningnanmycin; MST, Microscale thermophoresis; TMV-CP, Tobacco mosaic virus coat protein; MDA, Malondialdehyde; SOD, Superoxide dismutase.

\* Corresponding author.

E-mail address: [wxue@gzu.edu.cn](mailto:wxue@gzu.edu.cn) (W. Xue).

<https://doi.org/10.1016/j.arabjc.2024.105944>

Received 23 June 2024; Accepted 30 July 2024

Available online 31 July 2024

1878-5352/© 2024 The Author(s). Published by Elsevier B.V. on behalf of King Saud University. This is an open access article under the CC BY-NC-ND license (<http://creativecommons.org/licenses/by-nc-nd/4.0/>).

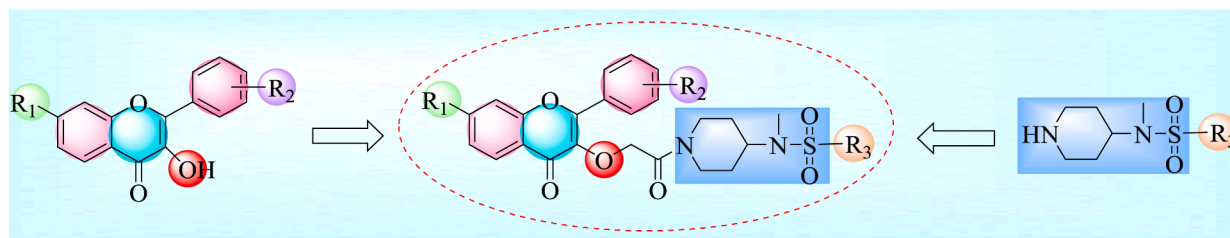


Fig. 1. Design of target compounds.

(Wei et al., 2023; Zhou et al., 2018) and insecticidal (Jing et al., 2024) biological activities.

A series of flavonol derivatives containing piperidine sulfonamide were synthesized by using flavonol as the lead compound and structurally modified by active splicing method (Fig. 1).

## 2. Materials and methods

### 2.1. Chemicals and instruments

Thin layer chromatography was performed with WFH-203B UV analyzer (Shanghai Jingke, China). The reagents and solvents used are analytical grade and are used directly without the need for further purification and drying. The nuclear magnetic resonance (NMR) spectrum was acquired by a Bruker 400 NMR instrument (Bruker Co., Germany). High resolution mass spectrometry (HRMS) was obtained using the Thermo Scientific Q Exactive instrument (Thermo Scientific, USA). The solvent is mass spectrum methanol. The melting point was determined by XT-4 binocular microscope without correction (Beijing Science and Technology Instrument Co, LTD, China). Malondialdehyde (MDA) test kit and Active oxygen species (SOD) test kit was purchased (Beijing Solarbio Technilgy Co, LTD, China).

### 2.2. Synthesis of compounds

#### 2.2.1. Synthesis of intermediate 1–2

The reaction of *p*-hydroxyacetophenone (7.34 mmol) and substituted benzaldehyde (7.34 mmol) in the presence of NaOH (22.12 mmol) was

carried out at room temperature in a 500 mL round-bottom flask with anhydrous ethanol as the solvent. After the reaction, the product was poured into ice water, the pH was adjusted to neutral by adding dilute hydrochloric acid, and the solid was precipitated, filtrate and dry to obtain intermediate 1. Intermediate 1 (4.20 mmol) was added with NaOH (16.79 mmol) and H<sub>2</sub>O<sub>2</sub> (25.18 mmol), anhydrous methanol as solvent, the reaction at room temperature in 250 mL round bottom flask, after the reaction, the product into ice-cold water, also add HCl adjust pH to neutral, solid precipitation, filtration, drying, get intermediate 2.

#### 2.2.2. Synthesis of intermediate 3–5

Triethylamine (5.77 mmol) was added to substituted sulfonyl chloride (5.25 mmol) and 1-*tert*-butoxycarbonyl 4-methylaminopiperidine (5.77 mmol), and the reaction was performed in a 100 mL round-bottom flask containing methylene chloride solvent for 3 h in an ice bath. After the reaction, the reaction was extracted in methylene chloride solvent, get intermediate 3. Intermediate 3 (2.71 mmol) was added with HCl (32.57 mmol) in methanol solution at 80°C for reflux for 8 h, Boc was removed, and after the reaction, it was directly steamed under pressure, get intermediate 4. Intermediate 4 (5.22 mmol) reacted with chloroacetyl chloride (10.43 mmol) in an ice bath of dichloromethane solvent. After the reaction, intermediate 5 was extracted by dichloromethane solvent.

#### 2.2.3. Synthesis of Z1–Z23

Intermediates 2 (2.42 mmol) and K<sub>2</sub>CO<sub>3</sub> (4.85 mmol) were first stirred in DMF solvent at room temperature for 0.5 h, and then intermediates 5 (2.42 mmol) were added, and then reflow for 2–3 h at

Table 1

Antiviral activities of the target compounds against TMV at 500 μg/mL *in vivo*.

Compounds	R <sub>1</sub>	R <sub>2</sub>	R <sub>3</sub>	Curative (%) <sup>a</sup>	Protection (%) <sup>a</sup>	Inactivation (%) <sup>a</sup>
Z1	-OCH <sub>3</sub>	2-OCH <sub>3</sub>	Ph	61.5 ± 3.8	66.3 ± 1.7	64.5 ± 4.8
Z2	-OCH <sub>3</sub>	2-OCH <sub>3</sub>	4-F-Ph	63.2 ± 1.5	62.5 ± 2.9	58.7 ± 3.7
Z3	-OCH <sub>3</sub>	4-Br	Ph	55.7 ± 5.4	67.4 ± 5.4	56.0 ± 3.5
Z4	-OCH <sub>3</sub>	4-Cl	Ph	62.1 ± 3.8	80.2 ± 0.7	55.5 ± 4.0
Z5	-OCH <sub>3</sub>	4-OCH <sub>3</sub>	4-Cl-Ph	68.1 ± 3.0	78.5 ± 1.7	63.7 ± 0.8
Z6	-OCH <sub>3</sub>	4-OCH <sub>3</sub>	4-NO <sub>2</sub> -Ph	77.0 ± 2.9	79.4 ± 3.5	82.3 ± 2.2
Z7	-OCH <sub>3</sub>	4-Br	4-NO <sub>2</sub> -Ph	64.0 ± 2.6	65.0 ± 2.6	66.4 ± 3.4
Z8	-OCH <sub>3</sub>	4-F	4-Cl-Ph	52.2 ± 1.4	72.5 ± 4.4	65.2 ± 5.7
Z9	-OCH <sub>3</sub>	4-OCH <sub>3</sub>	ethyl	59.6 ± 5.5	57.0 ± 3.2	51.9 ± 2.5
Z10	-OCH <sub>3</sub>	4-Cl	ethyl	66.4 ± 4.1	63.0 ± 3.4	54.9 ± 4.7
Z11	H	2-OCH <sub>3</sub>	4-Cl-Ph	66.6 ± 1.8	52.3 ± 4.6	67.8 ± 2.0
Z12	H	3-CH <sub>3</sub>	4-Cl-Ph	71.7 ± 4.0	57.1 ± 2.0	58.2 ± 4.7
Z13	H	3-CH <sub>3</sub>	ethyl	64.5 ± 3.9	71.9 ± 2.1	45.5 ± 2.1
Z14	H	2-OCH <sub>3</sub>	4-F-Ph	70.2 ± 3.1	55.7 ± 5.1	51.0 ± 3.5
Z15	H	4-CH <sub>3</sub>	4-F-Ph	68.9 ± 2.3	65.0 ± 5.2	21.9 ± 2.4
Z16	H	2-Br	4-CH <sub>3</sub> -Ph	54.3 ± 3.4	50.9 ± 4.9	53.9 ± 2.3
Z17	H	2-Br	ethyl	65.8 ± 2.0	55.7 ± 4.2	55.8 ± 0.3
Z18	H	4-OCH <sub>3</sub>	4-CH <sub>3</sub> -Ph	57.3 ± 4.7	72.0 ± 4.1	66.8 ± 5.2
Z19	H	4-CH <sub>3</sub>	4-CF <sub>3</sub> -Ph	68.0 ± 1.7	35.2 ± 1.5	67.7 ± 0.9
Z20	H	4-Cl	4-CF <sub>3</sub> -Ph	56.7 ± 3.2	63.6 ± 5.7	77.3 ± 4.9
Z21	H	4-CH <sub>3</sub>	Ph	78.5 ± 3.3	73.1 ± 1.5	55.9 ± 1.2
Z22	H	4-OCH <sub>3</sub>	Ph	75.0 ± 2.8	51.7 ± 0.8	80.0 ± 2.2
Z23	H	3-F	4-NO <sub>2</sub> -Ph	62.1 ± 1.6	56.5 ± 3.9	52.6 ± 1.9
Flavonol	-OCH <sub>3</sub>	4-OCH <sub>3</sub>	–	25.3 ± 4.0	38.4 ± 5.2	–
NNM <sup>b</sup>	–	–	–	62.5 ± 2.4	67.1 ± 2.8	91.8 ± 2.6

<sup>a</sup> Values are mean ± SD of three replicates. <sup>b</sup> Commercial antiviral agents ningnanmycin(NNM).

**Table 2**  
The EC<sub>50</sub> values of several target compounds against TMV.<sup>a</sup>

Activity	Compounds	Regression equation	r	EC <sub>50</sub> (μg/mL)
Curative activity	Z6	y = 0.9990x + 2.9680	0.9846	108.2
	Z21	y = 0.9614x + 3.0335	0.9816	111.0
	Z22	y = 1.0372x + 2.9137	0.9846	102.7
	NNM <sup>b</sup>	y = 1.0685x + 2.4308	0.9937	253.8
Protective activity	Z4	y = 1.0471x + 2.8146	0.9846	122.2
	Z5	y = 1.0103x + 2.8414	0.9880	136.9
	Z6	y = 1.1013x + 2.7932	0.9885	100.9
	Z21	y = 0.9842x + 2.9425	0.9871	123.2
	NNM <sup>b</sup>	y = 0.9920x + 2.7545	0.9862	203.7

<sup>a</sup> Average of three replicates. <sup>b</sup> Commercial antiviral agents (NNM).

100°C, after the reaction, the solid was cooled to indoor temperature, and the solid was separated and purified by column chromatography (petroleum ether: ethyl acetate = 3:1, v/v) to obtain Z1-Z23.

### 3. Antiviral bioassays

#### 3.1. Anti-TMV activity test of Z1-Z23

The activity of Z1-Z23 against TMV was determined by the half-leaf blip method at a concentration of 500 μg/mL. The commercial drug NNM was used as a positive control to test the activity of anti-TMV *in vivo*, including curative activity, protective activity and inactivation activity. The tobacco seedlings with a growth cycle of 4 weeks were used

in the experiment, with left and right symmetry and uniform size of *Nicotiana glutinosa* (*N. glutinosa*). The preliminary screening results are shown in Table 1. On this basis, the EC<sub>50</sub> values of the compounds against TMV are further tested, as shown in Table 2. The specific experimental methods have been provided in the auxiliary materials.

#### 3.2. Microscale thermophoresis (MST) test

According to the MST test method (Wang et al., 2023b; Cao et al., 2023b) in the literature, the correlation between Z6, Z15 and Z21 with TMV-CP was tested respectively. The specific test method has been given in the supporting material.

#### 3.3. Molecular docking experiment

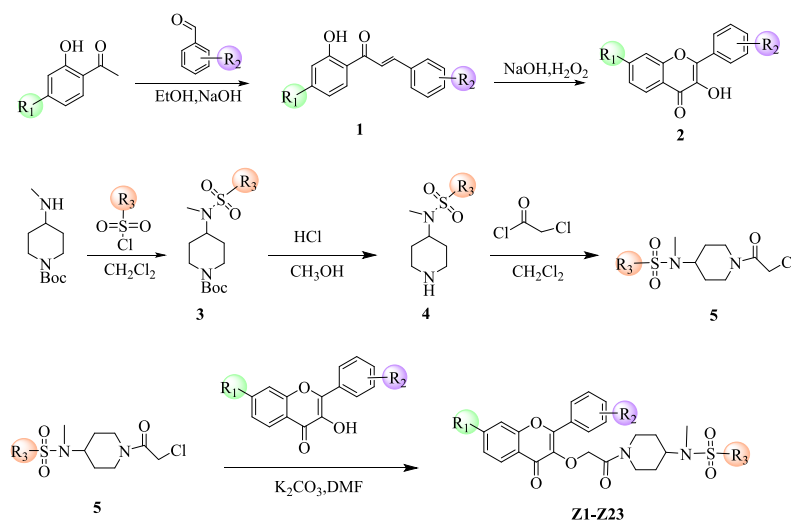
In order to further study the binding mode of the target compound with TMV-CP (PDB code:1EI7) at the molecular level, Z6, Z15 and Z21 were selected to perform molecular docking with TMV-CP in Discovery Studio software according to the method reported in literature (Xing et al., 2023). In supporting material describes the specific experimental methods.

#### 3.4. Biological safety of Z6

In order to study the effect of Z6 on tobacco seeds and seedlings, with the same growth cycle, different concentrations of Z6 were selected for spraying (Lu et al., 2024).

#### 3.5. Chlorophyll content test

The presence of chlorophyll lays the foundation for plant photosynthesis (Wei et al., 2019). Literature reports have indicated that the TMV infection can impact changes in plant chlorophyll content (Liu et al., 2022; Luo et al., 2023). Therefore, the variations in chlorophyll *a*, chlorophyll *b*, and total chlorophyll content of tobacco leaves after



Z1: R<sub>1</sub>=-OCH<sub>3</sub>, R<sub>2</sub>=2-OCH<sub>3</sub>, R<sub>3</sub>=Ph  
 Z2: R<sub>1</sub>=-OCH<sub>3</sub>, R<sub>2</sub>=2-OCH<sub>3</sub>, R<sub>3</sub>=4-F-Ph  
 Z3: R<sub>1</sub>=-OCH<sub>3</sub>, R<sub>2</sub>=4-Br, R<sub>3</sub>=Ph  
 Z4: R<sub>1</sub>=-OCH<sub>3</sub>, R<sub>2</sub>=4-Cl, R<sub>3</sub>=Ph  
 Z5: R<sub>1</sub>=-OCH<sub>3</sub>, R<sub>2</sub>=4-OCH<sub>3</sub>, R<sub>3</sub>=4-Cl-Ph  
 Z6: R<sub>1</sub>=-OCH<sub>3</sub>, R<sub>2</sub>=4-OCH<sub>3</sub>, R<sub>3</sub>=4-NO<sub>2</sub>-Ph  
 Z7: R<sub>1</sub>=-OCH<sub>3</sub>, R<sub>2</sub>=4-Br, R<sub>3</sub>=4-NO<sub>2</sub>-Ph  
 Z8: R<sub>1</sub>=-OCH<sub>3</sub>, R<sub>2</sub>=4-F, R<sub>3</sub>=4-Cl-Ph  
 Z9: R<sub>1</sub>=-OCH<sub>3</sub>, R<sub>2</sub>=4-OCH<sub>3</sub>, R<sub>3</sub>=ethyl  
 Z10: R<sub>1</sub>=-OCH<sub>3</sub>, R<sub>2</sub>=4-Cl, R<sub>3</sub>=ethyl  
 Z11: R<sub>1</sub>=H, R<sub>2</sub>=2-OCH<sub>3</sub>, R<sub>3</sub>=4-Cl-Ph  
 Z12: R<sub>1</sub>=H, R<sub>2</sub>=3-CH<sub>3</sub>, R<sub>3</sub>=4-Cl-Ph  
 Z13: R<sub>1</sub>=H, R<sub>2</sub>=3-CH<sub>3</sub>, R<sub>3</sub>=ethyl  
 Z14: R<sub>1</sub>=H, R<sub>2</sub>=2-OCH<sub>3</sub>, R<sub>3</sub>=4-F-Ph  
 Z15: R<sub>1</sub>=H, R<sub>2</sub>=4-CH<sub>3</sub>, R<sub>3</sub>=4-F-Ph  
 Z16: R<sub>1</sub>=H, R<sub>2</sub>=2-Br, R<sub>3</sub>=4-CH<sub>3</sub>-Ph  
 Z17: R<sub>1</sub>=H, R<sub>2</sub>=2-Br, R<sub>3</sub>=ethyl  
 Z18: R<sub>1</sub>=H, R<sub>2</sub>=4-OCH<sub>3</sub>, R<sub>3</sub>=4-CH<sub>3</sub>-Ph  
 Z19: R<sub>1</sub>=H, R<sub>2</sub>=4-CH<sub>3</sub>, R<sub>3</sub>=4-CF<sub>3</sub>-Ph  
 Z20: R<sub>1</sub>=H, R<sub>2</sub>=4-Cl, R<sub>3</sub>=4-CF<sub>3</sub>-Ph  
 Z21: R<sub>1</sub>=H, R<sub>2</sub>=4-CH<sub>3</sub>, R<sub>3</sub>=Ph  
 Z22: R<sub>1</sub>=H, R<sub>2</sub>=4-OCH<sub>3</sub>, R<sub>3</sub>=Ph  
 Z23: R<sub>1</sub>=H, R<sub>2</sub>=3-F, R<sub>3</sub>=4-NO<sub>2</sub>-Ph

**Scheme 1.** Synthetic route of the target compounds Z1-Z23.

treatment with **Z6** were further investigated to elucidate its mechanism of action. Specific experimental methods are detailed in the [supporting materials](#).

### 3.6. Malondialdehyde (MDA) content test

MDA is a biomarker produced by lipid peroxidation and intracellular oxidative stress. The content in MDA can indicate the degree of lipid peroxidation in cell membranes and the extent of membrane damage (Heath and Packer, 2022; Gong et al., 2024b). Therefore, the alteration in MDA content in tobacco leaves treated with **Z6** was chosen for further investigation into its mechanism of action. Specific experimental methods are detailed in the [supporting materials](#).

### 3.7. Defense enzyme activity assay

SOD is an antioxidant enzyme that converts superoxide radicals in plant cells into hydrogen peroxide ( $H_2O_2$ ) and oxygen molecules ( $O_2$ ), thus protecting cells from damage (Hunter et al., 1997). Accordingly, the change in SOD activity in tobacco leaves treated with **Z6** was recorded to further study its mechanism of action. Specific experimental methods are described in the [supporting materials](#).

## 4. Results and discussion

### 4.1. Chemistry

The synthesis pathway of the target compound has been given in [Scheme 1](#), and the specific spectral characterization data of **Z1-Z23** are given in the [supporting information](#).

### 4.2. Virus activity analysis

The resistance test of **Z1-Z23** to TMV at 500  $\mu\text{g}/\text{mL}$  concentration was determined, and the commercial drug NNM was used as a positive control. The preliminary screening data were shown in [Table 1](#). The curative activities of **Z5, Z6, Z12, Z14, Z15, Z19, Z21** and **Z22** on TMV were 68.1, 77.0, 71.7, 70.2, 68.9, 68.0, 78.5 and 75.0 %, respectively, which were superior to the control drug NNM (62.5 %). The protective activities of **Z4, Z5, Z6, Z8, Z13, Z18** and **Z21** against TMV were 80.2, 78.5, 79.4, 72.5, 71.9, 72.0 and 73.1 %, which were superior to the control drug NNM (67.1 %).

Based on the analysis of the activity data in [Table 1](#), it was found that the different structure of substituents structures also had a certain influence on the anti-TMV activity of the compound. Specifically, when substituents  $R_1 = -\text{OCH}_3$ ,  $R_2 = 4\text{-OCH}_3$ , the curative and protective activity of the target compound is higher than that of the electron-donating group when  $R_3$  is a strong electron-withdrawing group. For example, Curative and protective activity of **Z6** ( $R_3 = 4\text{-NO}_2\text{-Ph}$ ) > **Z5** ( $R_3 = 4\text{-Cl-Ph}$ ) > **Z9** ( $R_3 = \text{ethyl}$ ). In summary, **Z6** ( $R_1 = -\text{OCH}_3$ ,  $R_2 = 4\text{-OCH}_3$ ,  $R_3 = 4\text{-NO}_2\text{-Ph}$ ) exhibits good inhibitory activity in both curative and protection. The leaf characterization of **Z6** and NNM against TMV is shown in [Fig. 2](#).

### 4.3. Binding ability of **Z6** and NNM to TMV-CP

The [Fig. 3](#) shows the MST results of **Z6, Z15, Z21** and tobacco Mosaic virus coat protein (TMV-CP). The  $K_d$  value can be used to evaluate the binding affinity with TMV-CP. The  $K_d$  values of the three compounds binding to TMV-CP were  $0.4651 \pm 0.1227$ ,  $27.3606 \pm 7.4426$  and  $0.9720 \pm 0.4015 \mu\text{mol}/\text{L}$ , respectively. The results showed that the binding ability of **Z6** to TMV-CP was better than that of **Z15** and **Z21**, further suggesting its good antiviral activity.

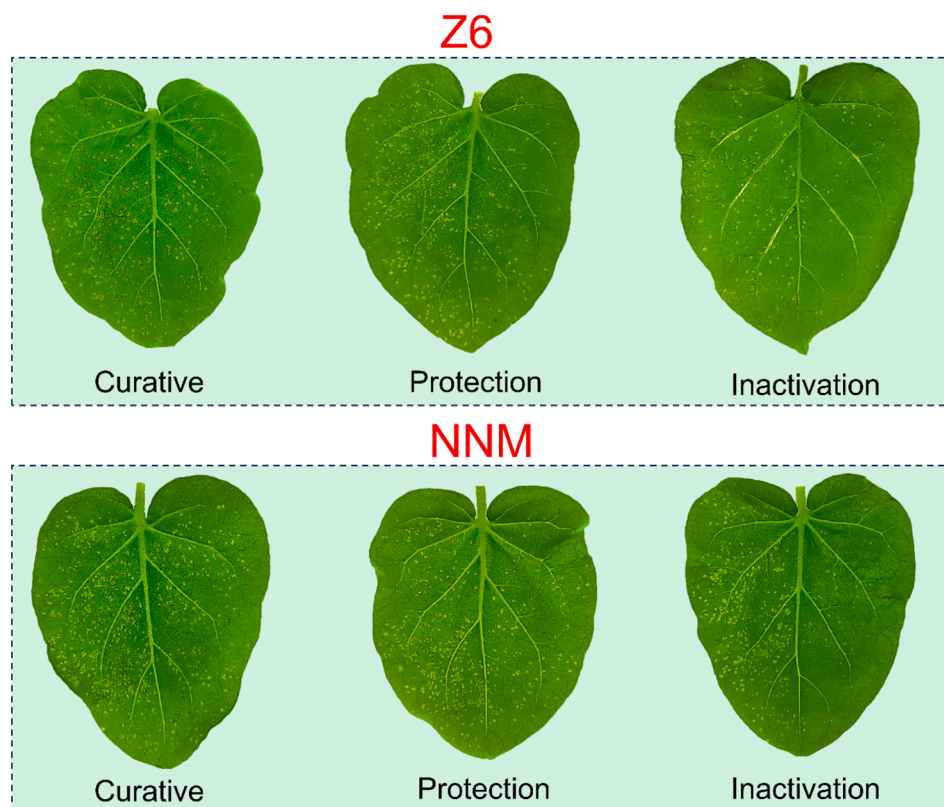


**Fig. 2.** Phenotypic study of TMV infection in tobacco treated with **Z6** and NNM (left leaf: untreated with compound; right leaf: treated with compound).

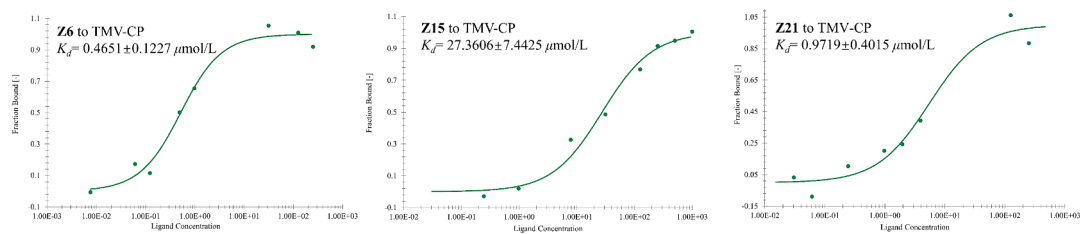


Fig. 3. Microscale thermophoresis (MST) of Z6, Z15 and Z21.

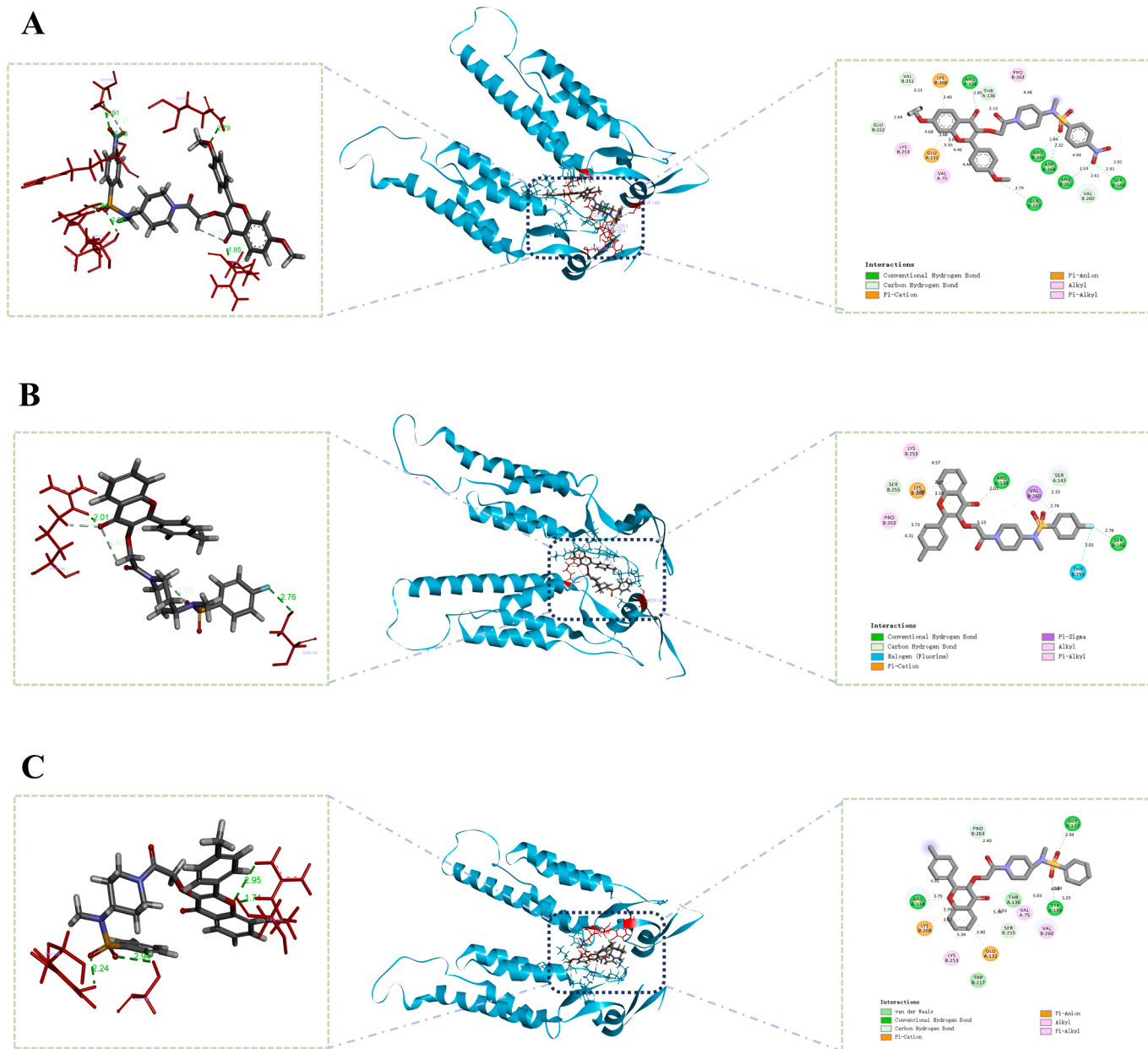


Fig. 4. The binding mode of Z6(A), Z15(B) and Z21(C) docked with TMV-CP.

#### 4.4. Molecular docking of Z6 with TMV-CP

As shown in the Fig. 4, The results of molecular docking demonstrated the ability of Z6, Z15, and Z21 to establish hydrogen bonds with TMV-CP. However, there is variation in the amino acid residues involved in these interactions, with 6, 2, and 3 amino acids respectively. The

hydrogen bond lengths for the conserved amino acid residue ARG-134 are measured at 1.85 Å, 2.07 Å, and 3.79 Å for Z6, Z15, and Z21 respectively. Henceforth, the differences in anti-TMV activity among Z6, Z15 and Z21 may be attributed to their distinct binding affinities with TMV-CP. Z6 binds to TMV-CP amino acid residues through six conventional hydrogen bonds, The oxygen atoms on the phenyl nitro group of

substituent R<sub>3</sub> form hydrogen bonds with the TMV-CP amino acid residues ARG-261 (2.53 Å) and SER-146 (2.91 Å). The oxygen atom on the sulfonyl group forms hydrogen bonds with the TMV-CP amino acid residues ARG-341 (1.84 Å) and ASP-146 (2.32 Å). The oxygen atom on the methoxy group of the substituent R<sub>2</sub> forms a hydrogen bond with the TMV-CP amino acid residue GLN-257 (2.79 Å). The oxygen atom on the flavonol carbon–oxygen double bond forms a hydrogen bond with the TMV-CP amino acid residue ARG-134 (1.86 Å). In addition, Z6 interacts with nine other TMV-CP amino acid residues: (VAL-260, PRO-263, THR-136, LYS-253, VAL-75, LYS-26, GLU-131, GLU-222, and VAL-251). The experimental results further prove that Z6 has a good binding affinity with TMV-CP.

#### 4.5. Biological safety of Z6

As shown in the Fig. 5, Z6 and DMSO at concentrations of 250, 500 and 1000 µg/mL were sprayed on the seeds of *N. glutinosa*. It was found that the seed germination was almost unaffected. Similarly, sprays of Z6 and DMSO at concentrations of 250, 500, and 1000 µg/mL had almost no effect on the growth of *N. glutinosa* with the same growth cycle. The results indicated that Z6 had no significant effect on the germination or growth of the seeds, which proved that Z6 had a non-significant effect on plant growth and good biosafety.

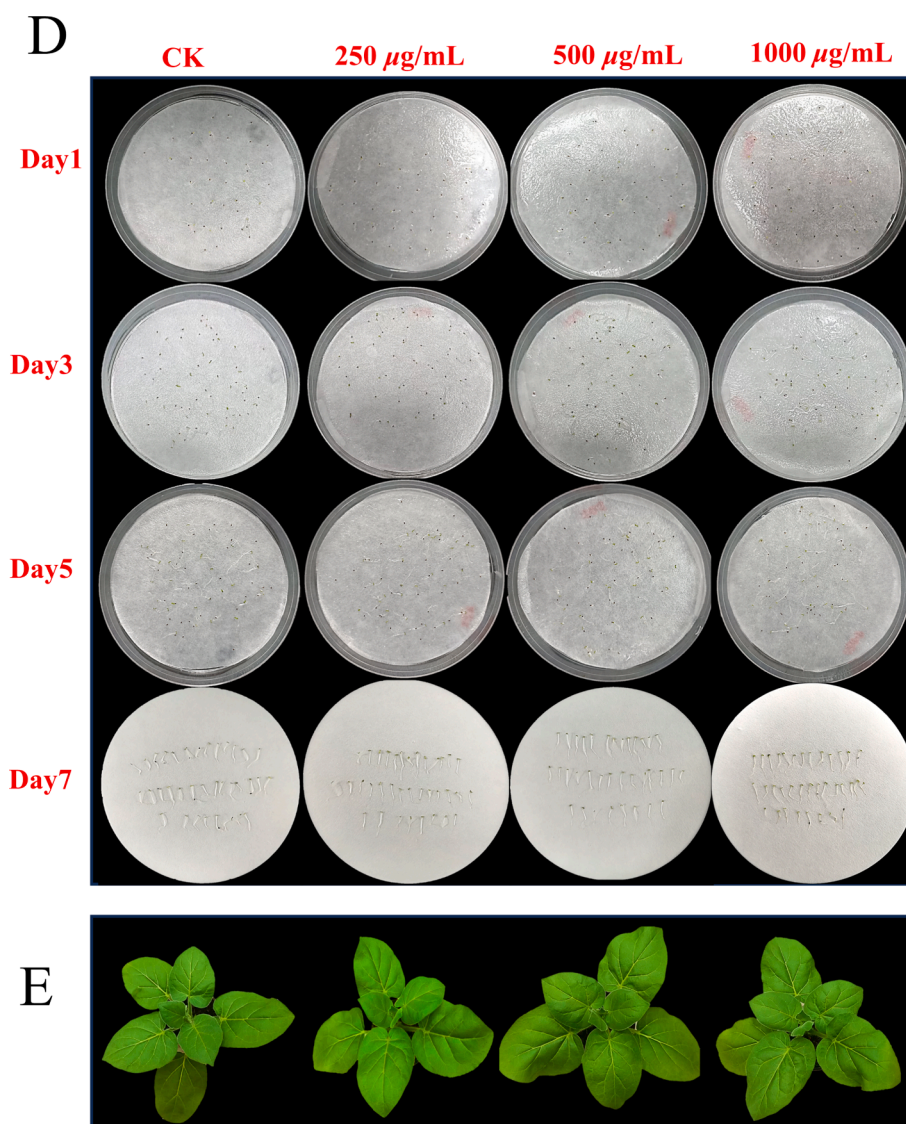


**Fig. 5.** Biological safety of Z6 (D) Photos of tobacco seeds soaked in Z6 solution of different concentrations for 1, 3, 5, and 7 d. (E) Photos taken after 7 d of growth of seedlings sprayed with different concentrations of Z6 solution.

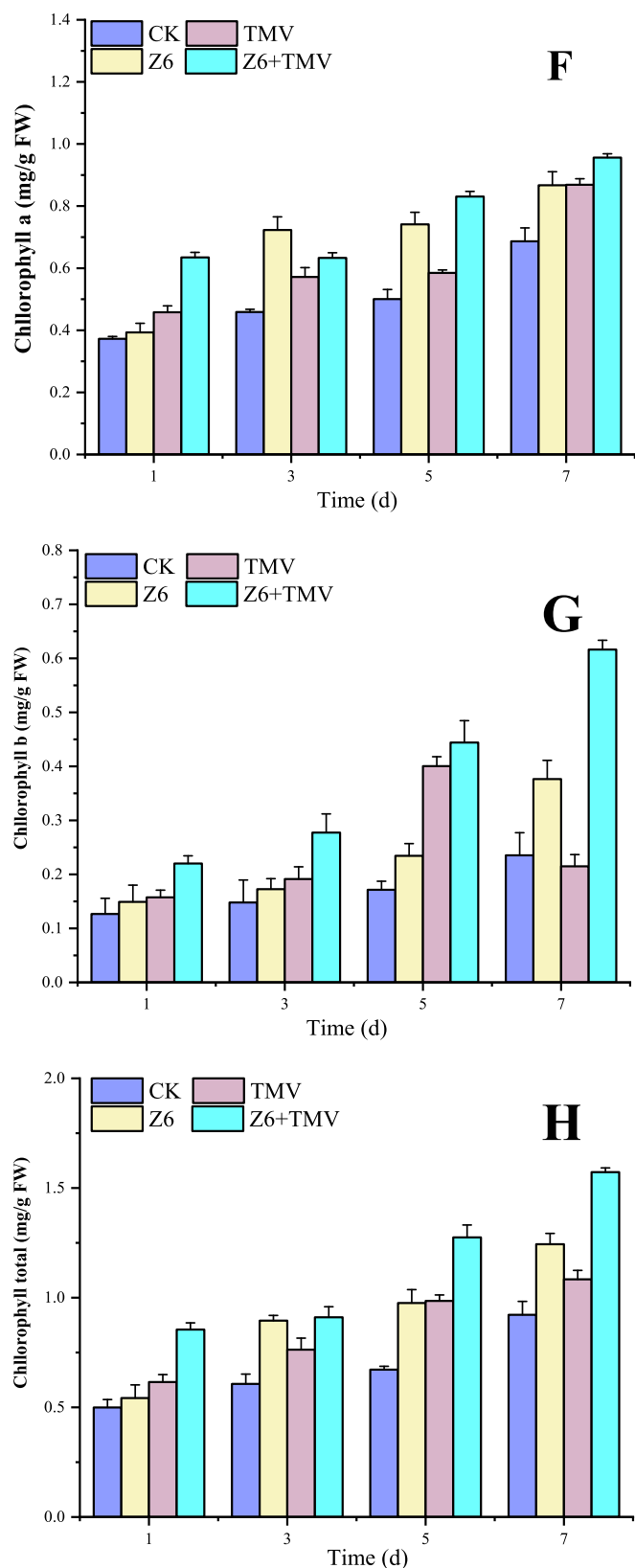


Fig. 6. Changes of chlorophyll content in tobacco after Z6 treatment.

#### 4.6. Chlorophyll content of Z6

The change of chlorophyll content directly affects the progress of plant photosynthesis and is closely related to plant growth. It can be seen from the Fig. 6 that Z6 can change the content of chlorophyll in tobacco leaves to a certain extent. The chlorophyll content of tobacco leaves treated with Z6 was significantly higher than that of the blank control group, which proved that Z6 could promote the photosynthesis of plants to a certain extent and improve the ability of plants to anti-TMV.

#### 4.7. MDA content analysis of Z6

As shown in the Fig. 7, MDA content in treated tobacco leaves was measured after 1, 3, 5, and 7 d. MDA content was higher than that in healthy tobacco leaves after 3–7 d of TMV infection, indicating that TMV seriously damaged the integrity of cell membrane. However, the MDA content of tobacco leaves treated with Z6 was significantly lower than that of CK group, especially on the 7th day. With the aging of leaves, the phenomenon was more obvious, indicating that Z6 could inhibit membrane lipid peroxidation and membrane damage to a certain extent, thus resisting the infection of TMV.

#### 4.8. Defense enzyme activity of Z6

As shown in the Fig. 8, SOD enzyme activity in the blank group and drug group infected by TMV was higher than that in the blank group and drug group not infected by TMV, because the cell defense mechanism would be activated after TMV infection, thus increasing SOD activity. In general, SOD activity in drug group was higher than that in blank control group. It can be concluded that Z6 can improve SOD activity, promote SOD generation and eliminate  $O_2^-$  in cells to a certain extent. Thereby improving the disease resistance of the plant.

### 5. Conclusions

In summary, 23 flavonol derivatives containing piperidine sulfonamide were designed and synthesized in this paper, and their antiviral activities were evaluated, and Z6 was found to have good therapeutic and protective activities.  $EC_{50}$  values of 102.7 and 100.9  $\mu\text{g}/\text{mL}$  were better than those of commercial agents NNM (253.8 and 203.7  $\mu\text{g}/\text{mL}$ ). The results of MST and molecular docking showed that Z6 had a good binding force with TMV-CP, with a  $K_d$  value of 0.4651  $\mu\text{mol}/\text{L}$ , and it was bound to TMV-CP amino acid residues by six conventional hydrogen bonds. At the same time, Z6 has little effect on the germination and growth of tobacco seeds, and has good biosafety. To a certain extent, it can also increase chlorophyll content and promote plant photosynthesis. Leaves treated with Z6 can slow the increase of MDA content in plants, improve SOD enzyme activity to a certain extent, inhibit the damage to tobacco leaves, promote the generation of SOD and the clearance of  $O_2^-$  in cells. This improves the disease resistance of the plant. Therefore, Z6 is expected to be a potential antiviral agent in the future.

#### CRedit authorship contribution statement

**Zhiling Sun:** Writing – original draft, Visualization, Data curation, Conceptualization. **Wei Zeng:** Visualization, Formal analysis, Conceptualization. **Qing Zhou:** Software, Formal analysis, Conceptualization. **Yujiao Qiu:** Formal analysis, Conceptualization. **Yuzhi Hu:** Investigation, Formal analysis. **Jieyu Li:** Methodology, Formal analysis. **Hong Fu:** Investigation, Formal analysis. **Hongqian Zou:** Methodology, Formal analysis. **Wei Xue:** Conceptualization, Formal analysis, Visualization.

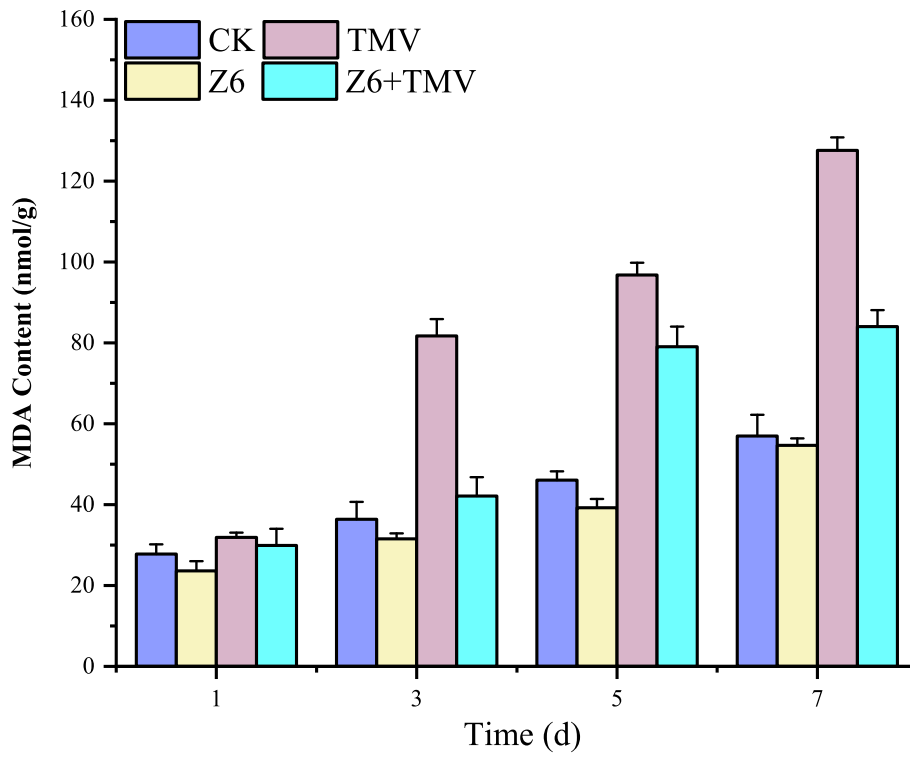


Fig. 7. Changes of MDA content in tobacco after Z6 treatment.

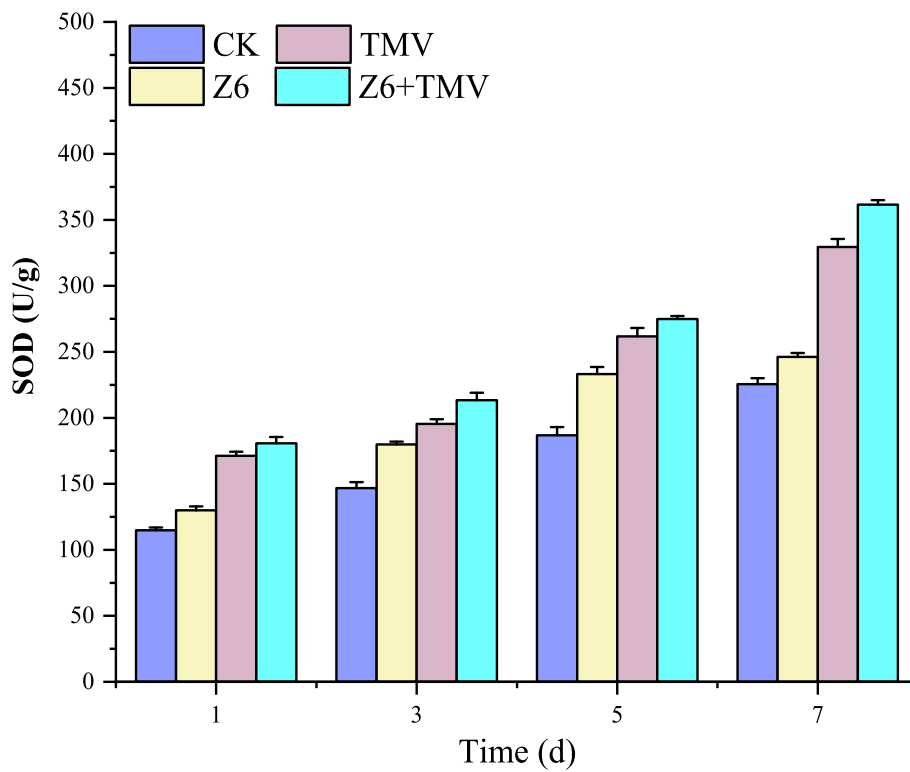


Fig. 8. Changes of SOD activity in tobacco after Z6 treatment.

## Declaration of competing interest

The authors declare that they have no known competing financial interests or personal relationships that could have appeared to influence the work reported in this paper.

## Acknowledgements

Authors gratefully acknowledge the Science Foundation of Guizhou Province (No. ZK2024008), The Key Research and Development Program of Hainan Province (No. ZDYF2024XDNY202).

## Appendix A. Supplementary data

Supplementary data to this article can be found online at <https://doi.org/10.1016/j.arabj.2024.105944>.

## References

- Aherne, S.A., O'Brien, N.M., 2002. Dietary flavonols: chemistry, food content, and metabolism. *Nutrition* 18 (1), 75–81. <https://doi.org/10.1006/enrs.2000.4224>.
- Borsari, C., Luciani, R., Pozzi, C., et al., 2016. Profiling of flavonol derivatives for the development of antitrypanosomatidic drugs. *J. Med. Chem.* 59 (16), 7598–7616. <https://doi.org/10.1021/acs.jmedchem.6b00698>.
- Cao, X., He, B.C., Liu, F., Zhang, Y.Q., Xing, L., Zhang, N., Zhou, Y.X., Gong, C.Y., Xue, W., 2023a. Design, synthesis and bioactivity of myricetin derivatives for control of fungal disease and tobacco mosaic virus disease. *RSC Adv.* 13 (10), 6459–6465. <https://doi.org/10.1039/d2ra08176h>.
- Cao, X., Liu, F., He, B.C., Xing, L., Zhang, Y.Q., Zhang, N., Xue, W., 2023b. Design, synthesis, bioactivity and mechanism of action of novel myricetin derivatives containing amide and hydrazide. *Arab. J. Chem.* 16 (4), 104588 <https://doi.org/10.1016/j.arabj.2023.104588>.
- Chen, Y., Luo, X., Wang, Y., Xing, Z., Peng, J., Chen, J., 2023. Design, synthesis and antibacterial activity of 1,3,4-Oxadiazole sulfones containing sulfonamide structure. *Chin. J. Org. Chem.* 43 (1), 274–284. <https://doi.org/10.6023/cjoc202204068>.
- Chen, M., Su, S.J., Zhou, Q., Tang, X.M., Liu, T.T., Peng, F., He, M., Luo, H., Xue, W., 2021. Antibacterial and antiviral activities and action mechanism of flavonoid derivatives with a benzimidazole moiety. *J. Saudi Chem. Soc.* 25 (2), 101194–101208. <https://doi.org/10.1016/j.jscs.2020.101194>.
- Ding, C., Pan, Y., Tan, C., 2020. Synthesis and biological activity of aryl thiazole piperidine amide compounds. *Chin. J. Org. Chem.* 40 (2), 528–535. <https://doi.org/10.6023/cjoc201907034>.
- Du, W.J., Yang, X.L., Song, Z.J., Wang, J.Y., Zhang, W.J., He, X., Zhang, R.Q., Zhang, C. F., Li, F., Yu, C.H., Wang, C.Z., Yuan, C.S., 2016. Antitumor activity of total flavonoids from daphne genkwa in colorectal cancer. *Phytother. Res.* 30 (2), 323–330. <https://doi.org/10.1002/ptr.5540>.
- Gong, C.Y., Meng, K.N., Sun, Z.L., Zeng, W., An, Y.S., Zou, H.Q., Qiu, Y.J., Liu, D., Xue, W., 2024b. Flavonol derivatives containing a quinazolinone moiety: design, synthesis, and antiviral activity. *Chem. Biodiversity.* 21 (2) <https://doi.org/10.1002/cbdv.202301737>.
- Gong, C.Y., Zhou, Y.X., Zhou, Q., Meng, K.N., Sun, Z.L., Zeng, W., Xue, W., 2024a. Novel flavonoid derivatives containing 1,2,4-triazolo [4,3-a] pyridine as potential antifungal agents: design, synthesis, and biological evaluation. *J. Saudi Chem. Soc.* 28 (2), 101797–101812. <https://doi.org/10.1016/j.jscs.2023.101797>.
- Heath, R.L., Packer, L., 2022. Photoperoxidation in isolated chloroplasts i. kinetics and stoichiometry of fatty acid peroxidation. *Arch. Biochem. Biophys.* 726 (125), 109248–109255. <https://doi.org/10.1016/j.abb.2022.109248>.
- Hunter, T., Bannister, W.H., Hunter, G.J., 1997. Cloning, expression, and characterization of two manganese superoxide dismutases from caenorhabditis elegans. *J. Biol. Chem.* 272 (2), 28652–28659. <https://doi.org/10.1074/jbc.272.45.28652>.
- Ilyas, R., Mareike, J.R., KatJa, R., Richert-Poggeler, Z.H., 2022. To be seen or not to be seen: latent infection by tobamoviruses. *Plants.* 11 (16), 2166–2179. <https://doi.org/10.3390/plants11162166>.
- Jing, T.T., Du, W.K., Qian, X.N., Wang, K., Luo, L.X., Zhang, X.Y., Deng, Y.N., Li, B., Gao, T., Zhang, M.T., Guo, D.Y., Jiang, H., Liu, Y.T., Schwab, W., Sun, X.L., Song, C. K., 2024. UGT89A1-mediated quercetin glucosylation is induced upon herbivore damage and enhances *Camellia sinensis* resistance to insect feeding. *Plant Cell Environ.* 47 (2), 682–697. <https://doi.org/10.1111/pce.14751>.
- Jones, R.A.C., 2021. Global plant virus disease pandemics and epidemics. *Plants.* 10 (2), 233–275. <https://doi.org/10.3390/plants10020233>.
- Kakigi, Y., Hakamatsuka, T., Icho, T., Goda, Y., Mochizuki, N., 2012. Comprehensive analysis of flavonols in ginkgo biloba products by Ultra-High-Performance liquid chromatography coupled with ultra-violet detection and time-of-flight mass spectrometry. *Biosci. Biotechnol. Biochem.* 76 (5), 1003–1007. <https://doi.org/10.1271/bbb.110873>.
- Keim, S.A., Alavanja, M.C.R., 2001. Pesticide use by persons who reported a high pesticide exposure event in the agricultural health study. *Environ. Res.* 85 (3), 256–259. <https://doi.org/10.1006/enrs.2000.4224>.
- Kosamu, I., Kaonga, C., Utembe, W., 2020. A critical review of the status of pesticide exposure management in malawi. *Int. J. Environ. Res.* 17 (18), 6727–6740. <https://doi.org/10.3390/ijerph17186727>.
- Landi, G., Linciano, P., Tassone, G., et al., 2020. High-resolution crystal structure of trypanosoma brucei pteridine reductase 1 in complex with an innovative tricyclic-based inhibitor. *Acta Cryst.* 76 (6), 558–564. <https://doi.org/10.1107/S2059798320004891>.
- Li, X., Chen, G.L., Zhang, X.J., Zhang, Q., Zheng, S.L., Wang, G.D., Chen, Q.H., 2016. A new class of flavonol-based anti-prostate cancer agents: design, synthesis, and evaluation in cell models. *Bioorg. Med. Chem. Lett.* 26 (17), 4241–4245. <https://doi.org/10.1016/j.bmcl.2016.07.050>.
- Li, Z.J., Hu, R.F., Zhang, C., Xiong, Y.K., Chen, K., 2022. Governmental regulation induced pesticide retailers to provide more accurate advice on pesticide use to farmers in China. *Pest Manage. Sci.* 78 (1), 184–192. <https://doi.org/10.1002/ps.6622>.
- Liu, P., Ning, Y., Zhou, Q., Mao, G., Niu, Z., 2015. One-dimensional rod-like tobacco mosaic virus self-assembly and applications. *Prog. Chem.* 27 (10), 1425–1434. <https://doi.org/10.7536/PC150412>.
- Liu, T.T., Peng, F., Zhu, Y., Cao, X., Wang, Q.F., Liu, F., Liu, L.W., Xue, W., 2022. Design, synthesis, biological activity evaluation and mechanism of action of myricetin derivatives containing thioether quinazolinone. *Arabian J. Chem.* 15 (8), 104019–104030. <https://doi.org/10.1016/j.arabj.2022.104019>.
- Lu, S., Liang, B., Hu, J., Liu, Y., Yang, F., Liu, J., 2024. Multidimensional response of dopamine nano-system for on-demand fungicides delivery: reduced toxicity and synergistic antibacterial effects. *Chem. Eng. J.* 482, 148990–149007. <https://doi.org/10.1016/j.cej.2024.148990>.
- Luo, W., Wang, K.Y., Luo, J.Y., Liu, Y.C., Tong, J.W., Qi, M.T., Jiang, Y., Wang, Y., Ma, Z. Q., Feng, J.T., Lei, B., Yan, H., 2023. Limonene anti-TMV activity and its mode of action. *Pestic. Biochem. Physiol.* 194, 105512–105523. <https://doi.org/10.1016/j.pestbp.2023.105512>.
- Mao, P., Deng, T.Y., Tian, J., Liu, Y., Xin, H., An, Y.S., Hu, Y.Z., Qin, Y.S., Xue, W., 2024. Design, synthesis, and antifungal activities of chalcone derivatives containing piperidine and sulfonamide moiety. *J. Saudi Chem. Soc.* 28 (1), 101791–101801. <https://doi.org/10.1016/j.jscs.2023.101791>.
- Meng, F., Yan, Z.X., Lu, Y.X., Wang, X.B., 2023. Design, synthesis, and antifungal activity of flavonoid derivatives containing thiazole moiety. *Chem. Pap.* 77 (2), 877–885. <https://doi.org/10.1007/s11696-022-02522-4>.
- Meseli, T., Dogan, S.D., Gunduz, M.G., Kokbudak, Z., Bogojevic, S.S., Noonan, T., VoJnovic, S., Wolber, G.J., Nikodinovic-Runic, 2021. Design, synthesis, antibacterial activity evaluation and molecular modeling studies of new sulfonamides containing a sulfathiazole moiety. *New J. Chem.* 45 (18), 8166–8177. <https://doi.org/10.1039/d1nj00150g>.
- Nimptsch, K., Zhang, X., Cassidy, A., Song, M., O'Reilly, E.J., Lin, J.H., Pischon, T., Rimm, E.B., Willett, W.C., Fuchs, C.S., Ogino, S., Chan, A.T., Giovannucci, E.L., Wu, K., 2016. Habitual intake of flavonoid subclasses and risk of colorectal cancer in 2 large prospective cohorts. *Am. J. Clin. Nutr.* 103 (1), 184–191. <https://doi.org/10.3945/ajcn.115.117507>.
- Pan, Z.J., Sun, G.Y., Zhang, A.Z., Fu, H., Wang, W.X., Ren, G.W., 2023. Tobacco disease detection model based on band selection. *Spectrosc. Spectral Anal.* 43 (4), 1023–1029. [https://doi.org/10.3964/j.issn.1000-0593\(2023\)04-1023-07](https://doi.org/10.3964/j.issn.1000-0593(2023)04-1023-07).
- Shamshad, H., Hafiz, A., Althagafi, I.I., et al., 2020. Characterization of the trypanosoma brucei pteridine reductase active-site using computational docking and virtual screening techniques. *Curr. Comput. Aided Drug Des.* 16 (5), 583–598. <https://doi.org/10.2174/1573409915666190827163327>.
- Shi, Z.H., Li, N.G., Tang, Y.P., Shi, Q.P., Zhang, W., Zhang, P.X., Dong, Z.X., Li, W., Zhang, X., Fu, H.A., Duan, J.A., 2014. Synthesis, biological evaluation and SAR analysis of O-alkylated analogs of quercetin for anticancer. *Bioorg. Med. Chem. Lett.* 24 (18), 4424–4427. <https://doi.org/10.1016/j.bmcl.2014.08.006>.
- Wang, F., Chen, Y., Pei, H., Zhang, J., Zhang, L., 2023a. Design, synthesis and antifungal activities of novel 1,2,4-oxadiazole derivatives containing piperidine. *Chin. J. Org. Chem.* 43 (8), 2826–2836. <https://doi.org/10.6023/cjoc202212015>.
- Wang, Q.F., Xing, L., Zhang, Y.Q., Gong, C.Y., Zhou, Y.X., Zhang, N., He, B.C., Xue, W., 2023b. Antiviral activity evaluation and action mechanism of myricetin derivatives containing thioether quinoline moiety. *Mol Divers.* <https://doi.org/10.1007/s11030-023-10631-9>.
- Wang, Y., Zhao, Z., Guo, R., Tang, Y., Guo, S., Xu, Y., Sun, W., Tu, H., Wu, J., 2024. Plant antiviral compounds containing pyrazolo [3,4-d] pyrimidine based on the systemin receptor model. *Arab. J. Chem.* 17 (8), 105849 <https://doi.org/10.1016/j.arabj.2024.105849>.
- Wei, C.L., Zhang, J., Shi, J., Gan, X.H., Hu, D.Y., Song, B.A., 2019. Synthesis, antiviral activity, and induction of plant resistance of indole analogues bearing dithioacetate moiety. *J. Agric. Food Chem.* 67 (50), 13882–13891. <https://doi.org/10.1021/acs.jafc.9b05357>.
- Wei, C.L., Yang, X., Shi, S.J., Bai, L., Hu, D.Y., Song, R.J., Song, B.A., 2023. 3-hydroxy-2-oxindole derivatives containing sulfonamide motif: synthesis, antiviral activity, and modes of action. *J. Agric. Food Chem.* 71 (1), 267–275. <https://doi.org/10.1021/acs.jafc.2c06881>.
- Wu, R., Liu, T., Wu, S.K., Li, H.D., Song, R.J., Song, B.A., 2022. Synthesis, antibacterial activity, and action mechanism of novel sulfonamides containing oxyacetal and pyrimidine. *J. Agric. Food Chem.* 70 (30), 9305–9318. <https://doi.org/10.1021/acs.jafc.2c02099>.
- Xing, L., Mao, P., He, B.C., Qin, Y.S., Meng, K.N., Zeng, W., Sun, Z.L., 2023. Design, synthesis, and antiviral activities of myricetin derivatives containing phenoxypyridine. *J. Saudi Chem. Soc.* 27 (6), 101751–101763. <https://doi.org/10.1016/j.jscs.2023.101751>.

- Zhang, X., Ma, H., Sun, T., Lei, P., Yang, X., Zhang, X., Ling, Y., 2019. Design, synthesis and fungicidal activity of novel piperidine containing cinnamaldehyde thiosemicarbazide derivatives. *Chin. J. Org. Chem.* 39 (10), 2965–2972. <https://doi.org/10.6023/cjoc201903031>.
- Zhang, N., Zeng, W., Zhou, Q., Sun, Z.L., Meng, K.N., Qin, Y.S., Hu, Y.Z., Xue, W., 2024. Design, synthesis, antibacterial and antiviral evaluation of chalcone derivatives containing benzoxazole. *Arab. J. Chem.* 17 (1), 105368–105381. <https://doi.org/10.1016/j.arabjc.2023.105368>.
- Zhou, Y.X., Sun, Z.L., Zhou, Q., Zeng, W., Zhang, M.H., Feng, S., Xue, W., 2024. Novel flavonol derivatives containing benzoxazole as potential antiviral agents: design, synthesis, and biological evaluation. *Mol. Diversity*. <https://doi.org/10.1007/s11030-023-10786-5>.
- Zhou, D.G., Xie, D.D., He, F.C., Song, B.A., Hu, D.Y., 2018. Antiviral properties and interaction of novel chalcone derivatives containing a purine and benzenesulfonamide moiety. *Bioorg. Med. Chem. Lett.* 28 (11), 2091–2097. <https://doi.org/10.1016/j.bmcl.2018.04.042>.